A dual biomimetic process for the selective aerobic oxidative coupling of primary amines using pyrogallol as a precatalyst. Isolation of the [5 + 2] cycloaddition redox intermediates

Martine Largeron, Patrick Deschamps, Karim Hammad, Maurice-Bernard Fleury

View Article Online
View Journal

Green Chemistry

Cutting-edge research for a greener sustainable future

Accepted Manuscript

This article can be cited before page numbers have been issued, to do this please use: M. Largeron, P. Deschamps, K. Hammad and M. Fleury, *Green Chem.*, 2020, DOI: 10.1039/C9GC03992A.

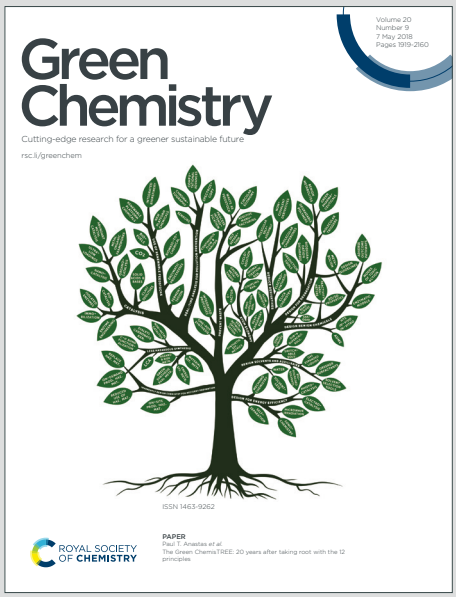

ROYAL SOCIETY OF CHEMISTRY

rsc.li/greenchem

View Article Online
DOI: 10.1039/C9GC03992A

ARTICLE

A dual biomimetic process for the selective aerobic oxidative coupling of primary amines using pyrogallol as a precatalyst. Isolation of the [5+2] cycloaddition redox intermediates

Received 00th January 20xx,
Accepted 00th January 20xx

DOI: 10.1039/x0xx00000x

Martine Largeron,*[a] Patrick Deschamps, [a] Karim Hammad [a] and Maurice-Bernard Fleury [a]

A bioinspired organocatalytic cascade reaction mimicking both purpurogallin biosynthesis and copper amine oxidases (CuAOs) activity is described, at room temperature under ambient air, for the activation of the α-C-H bond of primary amines. The reaction sequence uses low-cost commercially available pyrogallol as a precatalyst which undergoes an in situ oxidative self-processing step, resulting in its conversion into natural purpurogallin, a [5 + 2] cycloaddition redox intermediate. This is further involved in the CuAOs-like transamination mechanism for producing, under single turnover, the active biomimetic organocatalyst which mediates the selective oxidative coupling of primary amines, including the non-activated substrates of CuAOs. Without any metal cocatalyst or additives, the protocol gives access to cross-coupled imines as well as 1,2-disubstituted benzimidazoles. The isolation of not easily accessible [5+2] cycloaddition redox intermediates provides direct and clear evidence for the proposed dual biomimetic process.

Introduction

The concept of waste prevention is central, influencing all aspects of modern society. Due to the harmful effects of chemical waste on the environment, catalysis plays a major role in chemistry for achieving both environmental and economic objectives. By using catalysts to perform chemical transformations, the amounts of both reagents and waste generated are considerably reduced. In particular, biocatalysis, which refers to the use of enzymes for synthetic applications, and bioinspired catalysis, which involves chemical species mimicking certain features of enzymes, have been identified as green methodologies by taking the benefits of catalysis with significant improvements.[1] These naturally derived catalysts are generally highly active under mild conditions, at ambient temperature and pressure, and exhibit high selectivity. Given that they are found in biological systems, biocatalysts are relatively renewable, nontoxic and biodegradable. However, they may not catalyse the reaction with non-natural substrates or not yield the desired products. This activity gap has inspired chemists to introduce artificial cofactors into protein scaffolds leading to the development of artificial enzymes,[2] but also to design bioinspired catalysts.[3] These small molecules, which are devoid of protein scaffolds, have some advantages over naturally occurring biocatalysts as they may expand the scope of possible substrates and increase the scale of production. They are also useful for environmentally friendly catalytic chemistry, where it is important to avoid the use of toxic or expensive metal reagents, energy-consuming processing steps and undesirable solvents.

Copper amine oxidases (CuAOs) are a family of metalloenzymes which is involved in the metabolism of amines.[4] CuAOs couple the selective oxidation of unbranched primary amines to aldehydes with the reduction of dioxygen to hydrogen peroxide, through the synergistic action of a quinone-based organic cofactor, 2,4,5-trihydroxyphenylalanine quinone or topaquinone (TPQ) and a copper ion, which is not directly implicated in the amine oxidation step (Scheme 1).[5-7]

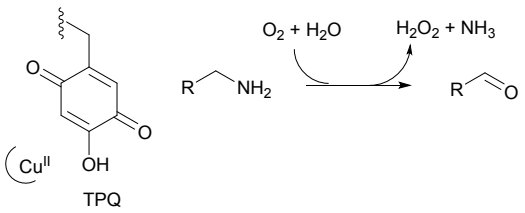

Scheme 1 Selective aerobic oxidation of primary amines to aldehydes mediated by CuAOs cofactors.

CuAOs have inspired considerable efforts to mimic their reactivity with synthetic quinone catalysts, earlier to demonstrate the transamination mechanism by which these enzymes operate,[8] while recent studies have focused on synthetic applications.[9] Thus, the aerobic oxidation of amines has been achieved with biomimetic or bioinspired quinone-based catalysts to accomplish cross-imination,[10] oxidative α-C-H functionalization,[11] cross-dehydrogenative coupling,[12] deaminative cross-coupling and N-nitrosation of amines.[13] Biomimetic catalytic systems promote selective aerobic oxidation of unbranched primary amines, at room

[a]Université de Paris, CiTCoM, UMR 8038, CNRS, F-75006 Paris, France.
E-mail : martine.largeron@parisdescartes.fr. https://orcid.org/0000-0002-1725-8118
†Electronic Supplementary Information (ESI) available: [details of any supplementary information available should be included here]. See DOI: 10.1039/x0xx00000x

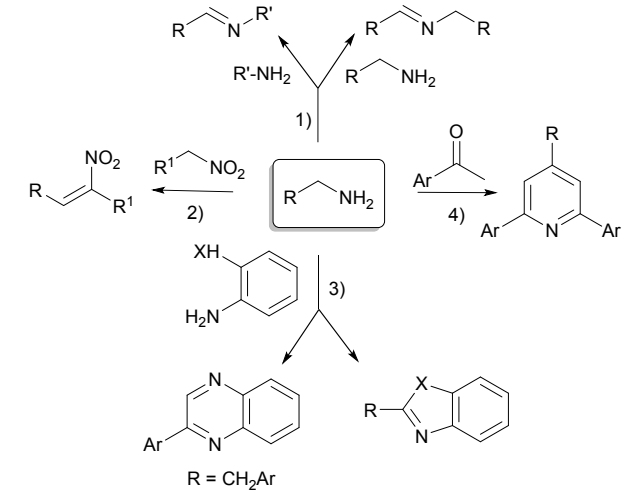

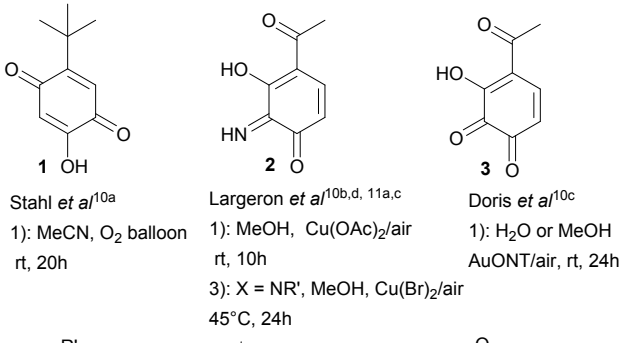

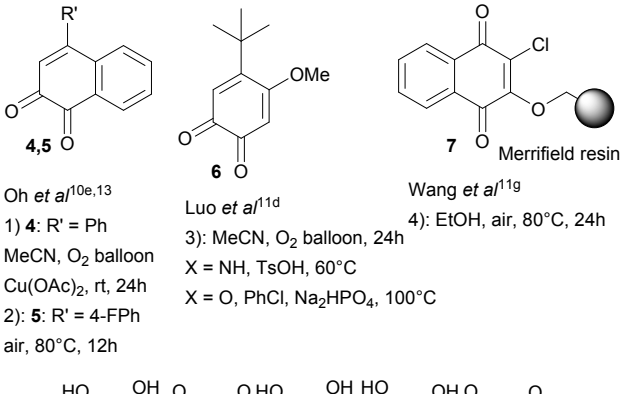

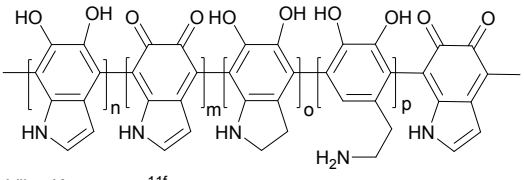

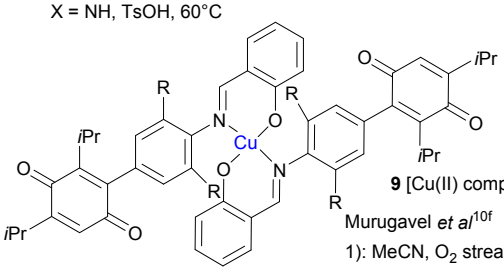

Scheme 2 Selective aerobic oxidation of unbranched primary amines mediated by biomimetic quinone-based catalysts **1**-**9**. Examples of synthetic applications.

temperature, without reacting with secondary and tertiary amines and follow a transamination mechanism reminiscent of that reported for natural CuAOs (Scheme 2),[10] while bioinspired catalysts surpass the activity of natural CuAOs by increasing the scope of substrates to α-branched,[12a,14] secondary[12a,13,15] and tertiary amines[12,13] following abiological pathways. Nevertheless, the procedures still suffer some drawbacks: 1) the majority of biomimetic catalysts has to be synthesized prior use affecting the economics as well as the eco-friendly nature of the methods; 2) when commercially available, the quinone catalysts are often expensive or require the cooperative action of additives such as metal co-catalyst. This may constitute a problem in the synthesis of medicinally relevant compounds due to the contamination of the final products by metal residues; 3) very few quinone-catalysed amine oxidation protocols are applicable to non-activated primary aliphatic amines, the natural substrates for CuAOs.

Recently, the concept of "second-order" biomimicry has been defined to describe a system in which in situ modification or processing of pre-catalyst components affords the active biomimetic catalyst, as opposed to "first-order" biomimicry, in which the active biomimetic catalyst is synthesized directly.[16] Obviously, "second-order" biomimicry introduces new opportunities for the discovery of efficient active biomimetic organocatalysts generated in situ from simple and low-cost precursors, without turning to chemical synthesis.

In a preliminary communication, we have recently reported the first example of "second-order" biomimicry for the selective aerobic oxidation of unbranched primary amines to imines under exceptionally mild conditions (Scheme 3).[17]

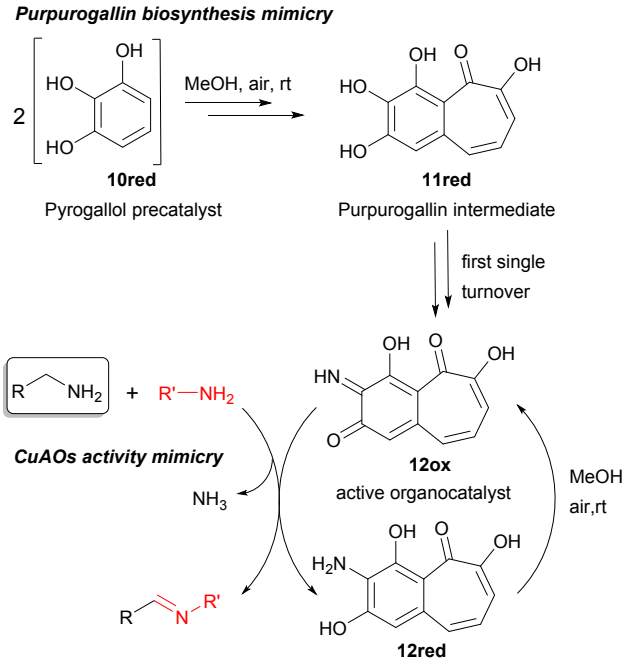

Scheme 3 Proposed "second-order" biomimicry for the aerobic oxidative cross-coupling of primary amines to imines.

This one-pot cascade reaction sequence, which mimics both purpurogallin biosynthesis and CuAOs activity, starts from commercially available low-cost pyrogallol **10red** as a precatalyst, allowing in situ formation of not easily accessible natural

purpurogallin (2,3,4,6-tetrahydroxy-5H-benzocyclohepten-5-one) **11red**. This is further engaged in the CuAOs-like transamination mechanism affording, under single turnover, the active biomimetic organocatalyst **12ox**, which mediates the oxidative coupling of primary amines under ambient air. However, the proposed reaction pathway was only based on control experiments and we were aware that a real proof of the transient presence of purpurogallin was highly desirable. In this full paper, we present the results of new experiments aimed at validating the "second-order" biomimetic process, through the isolation of [5+2] cycloaddition redox intermediates including purpurogallin.

Results and discussion

The limited availability of natural purpurogallin **11red** led us to examine its well-established biosynthesis, which involves the oxidative dimerization of pyrogallol **10red** generated from gallic acid **13**. Two molecules of *o*-quinone are engaged in a [5 + 2] cycloaddition reaction affording, after tautomerization reaction, the benzotropolone scaffold **14** (Scheme 4). Attack of water on the carbonyl bridge of **14** yields a carboxylic intermediate, which is prone to further oxidation and decarboxylation, leading to purpurogallin **11red**.[18] Accordingly, we chose to utilize **10red** as a precatalyst for generating **11red** in situ.

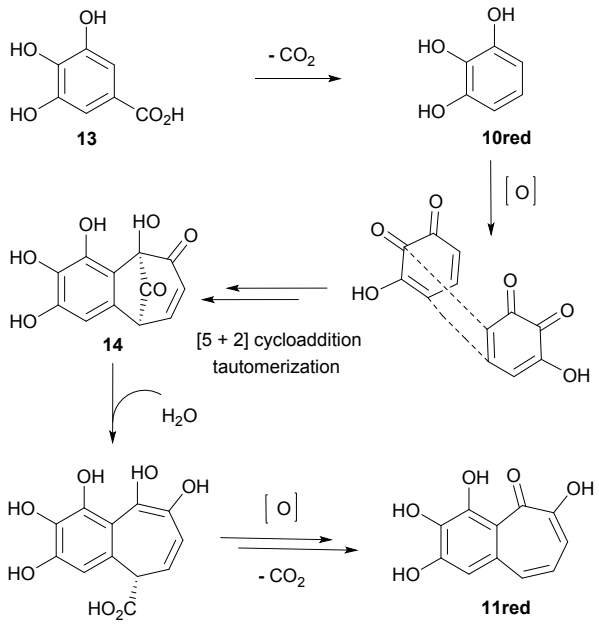

Scheme 4 Established biosynthesis of purpurogallin **11red**.

Early attempts to isolate **11red** as a key intermediate in the proposed dual bioinspired organocatalytic process were performed using benzylamine **15** as the amine substrate. Previous optimization studies had revealed that a combination of one equivalent of benzylamine with 0.04 equivalent of **10red** (4 mol% allowing the generation of 2 mol% of **11red**) was ideal for the reaction. Complete conversion of **15** into *N*-benzylidene-benzylamine **16** (see Scheme 7) was then observed after 24h, at room temperature, under ambient air, using MeOH as the solvent.[17] Under these experimental conditions, the reaction medium could contain no more than 2 mol% of **11red** which contrasted with the large excess of benzylamine utilized. Obviously, the low amount of **11red** susceptible to be formed in situ, combined with its very low solubility in organic media, would create serious problems in the course of the isolation procedure, especially during the column chromatography. So, we envisioned some modifications of our initial protocol. First, we changed **10red** to **17red**, because the isolation of the corresponding purpurogallin analogue **18red** should be facilitated by the presence of two benzyl groups (Scheme 5). To ensure that **17red** and **10red** behaved similarly, the aerobic catalytic oxidation of benzylamine **15** was performed under the optimal reaction conditions,[17] using **17red** as the starting material. The reaction proceeded smoothly and full conversion into imine **16** could be attained after a prolonged reaction time of 36h. Second, we decided to modify the molecular ratio between **17red** and amine **15** to facilitate the isolation of purpurogallin-like intermediate **18red** from the bulk solution. Accordingly, the reaction was carried out in MeOH, at room temperature, under ambient air, in the presence of one equivalent of **15** and 0.25 equivalent of **17red**. When 30% of **15** was converted to imine **16**, the reaction was stopped by addition of dry ice. After evaporation of the solvent and column chromatography, two [5 + 2] cycloaddition new redox products **18red** and **19red** were isolated in 5 and 15% yields, respectively (Scheme 5).

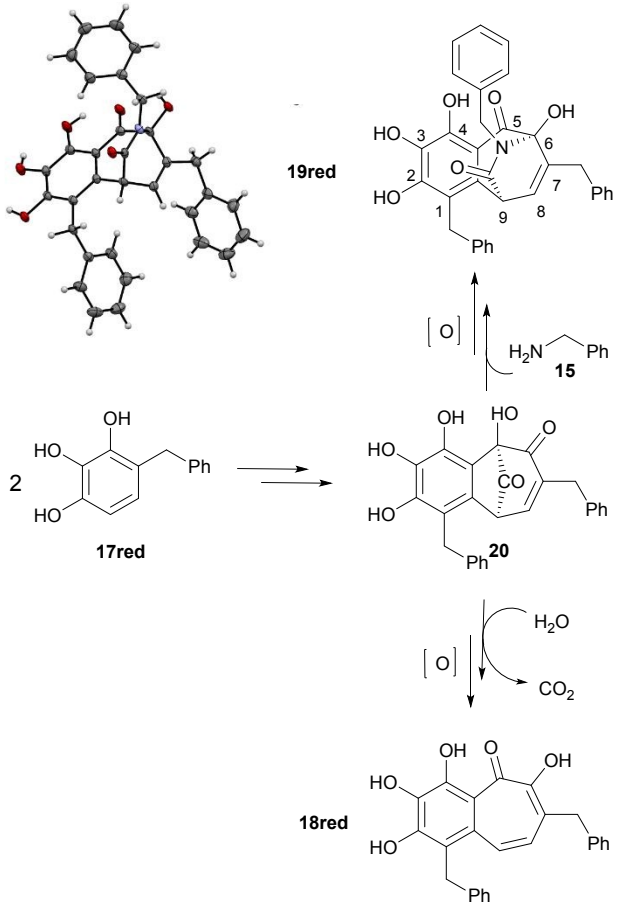

Scheme 5 [5 + 2] cycloaddition redox products **18red** and **19red** isolated during the aerobic oxidation of benzylamine mediated by **17red.** Ortep view of **19red**. Displacement ellipsoids are drawn at the 50% probability level.

The structure of **18red** was established on the basis of extensive spectroscopic data including 2D NMR experiments (See Experimental and ESI), while the X-Ray crystallographic data undoubtedly confirmed the proposed structure **19red** as a single diastereomer of relative configuration 6*R*,9*R* (Scheme 5 and Table S1).

From these results, it could be deduced that [5+2] cycloaddition redox intermediates could be formed in MeOH, under ambient air, starting from a pyrogallol derivative, in the presence of benzylamine. Note pyrogallol **17red** was stable in methanol under ambient aerobic conditions and did not produce spontaneously the aerobic dimerization product, purpurogallin **18red.** The presence of benzylamine was required for producing the monoanionic form of pyrogallol **17red** (pKa around 9) which was further oxidized to the *ortho*quinone redox species. Two molecules of *ortho*quinone were further engaged in the [5+2] cycloaddition reaction initiating the formation of purpurogallin **18red**. The latter would result from a nucleophilic attack of intermediate **20** (Scheme 5) by water, oxidation and decarboxylation steps, following a way which parallels that established for purpurogallin biosynthesis (Scheme 4). Interestingly, another [5+2] cycloaddition reaction product **19red** was also isolated. Its formation very likely would arise from a competitive nucleophilic attack of benzylamine **15** on the carbonyl group in the five-membered ring of intermediate **20**, resulting in a ring-opening reaction.[19] Subsequent oxidation step involving amide intermediate **21** would afford **22** which would rearrange into compound **19red** as proposed in Scheme 6.

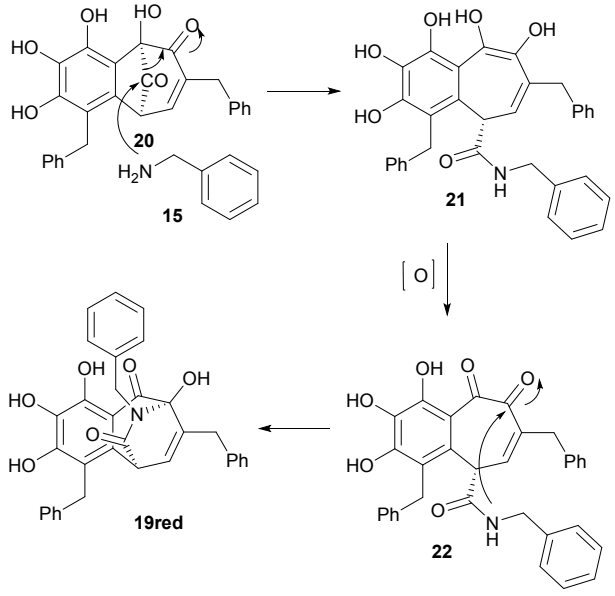

Scheme 6 Proposed reaction mechanism for the formation of compound **19red**.

At this stage, note that both compounds **18red** and **19red** displayed two features that we have previously observed with redox precursors of bioinspired quinone-based catalysts of the same series: first, the presence of a carbonyl group adjacent to the pyrogallol moiety; second, the presence of an active hydroxyl group (red OH in Scheme 7). This was found to be an essential component of the catalytic activity associated with enzymatic[7a,7d,8] and non-enzymatic catalytic systems[9c,10a-d,20] through the formation of a highly reactive H-bonded cyclic transition state (CTS) (see Scheme 8). Note we had also shown that the aerobic oxidation of 2-aminoresorcinol (4 mol%) produced a poorly reactive *o*-iminoquinone catalyst, that mainly decomposed to melanin-like polymers, giving only 5% of imine **16**.[17] When compared to highly reactive *o*-iminoquinone **2** (Scheme 2), this result confirmed the essential role of the acetyl group for successful operation of the catalytic process.[20c]

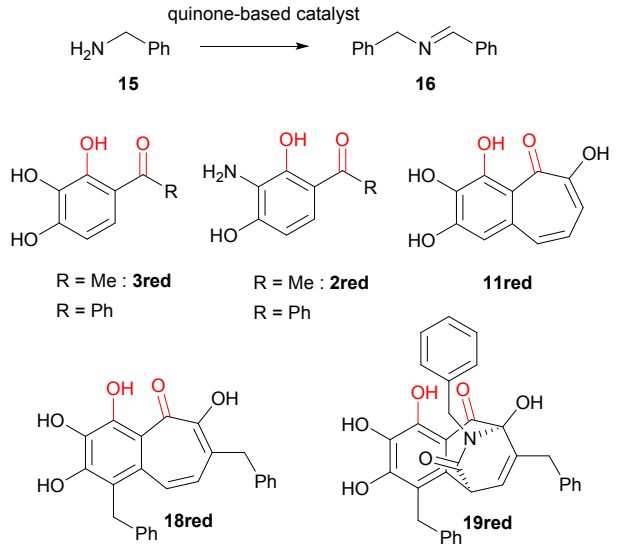

Scheme 7 Structural analogy between the redox precursors of bioinspired active quinone-based catalysts and products **18red** and **19red**.

Therefore, we were encouraged to consider that not only **18red** but also **19red**, could be involved in the aerobic catalytic oxidation of benzylamine **15** to imine **16**. Consequently, to clarify their respective role in supporting the catalytic efficiency, each compound (2 mol%) was separately tested in the presence of **15**, under the optimal reaction conditions.

After 36h, almost full conversion (87%) of **15** into **16** could be observed starting from **18red**, while the benzylamine conversion did not exceed 40% using **19red**. As a consequence, **18red** proved to be the better candidate for generating the quinone-based catalyst responsible for the high catalytic efficiency observed when compound **17red** was used as the starting material (full conversion after 36h). Then, the continuously low concentration of the in situ generated *o*-quinone species **18ox** (see Scheme 8) should protect it against the competitive formation of melanin-like polymers. Finally, **18red** exhibited a behaviour close to that already observed with natural purpurogallin **11red**.[17] Taking all together, **18red** was considered as the most effective [5+2] cycloaddition intermediate in the bioinspired aerobic oxidative cascade reaction sequence allowing the oxidation of primary amines to imines.

The second part of the reaction sequence concerns the CuAOs activity mimicry. Once again, we showed that α-branched primary amines such as *sec*-benzylamine were poor substrates for the biomimetic catalytic process (5-10% conversion), while secondary amines were not reactive at all. These results were fully in agreement with the enzymatic transamination mechanism which has been well

established through the utilization of bioinspired quinone-based catalytic systems (Scheme 8).[8,10,14a,20a,c]

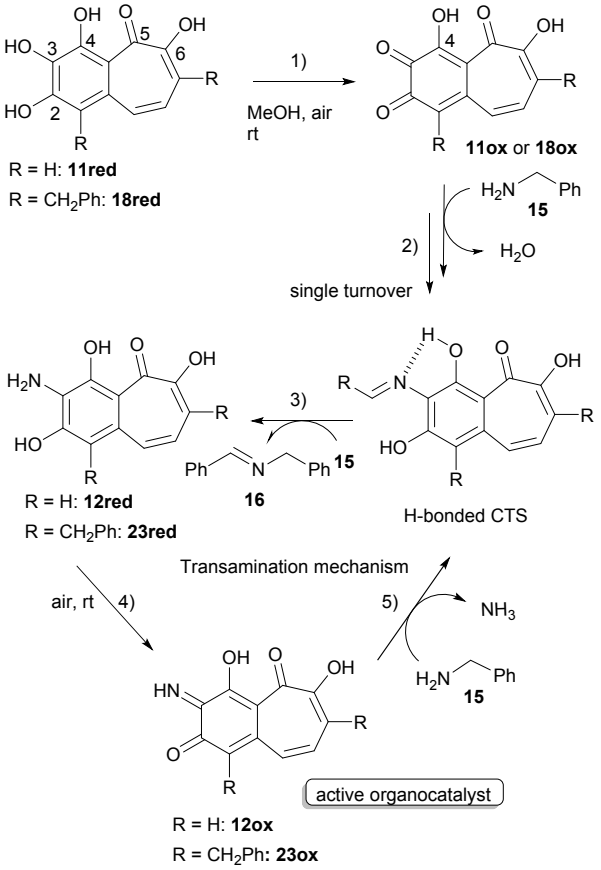

Scheme 8 Proposed transamination mechanism for the aerobic oxidation of primary amines to imines mediated by *o*-iminoquinone active organocatalyst **12ox** or **23ox**.

The presence of the benzotropolone scaffold not only favoured attack of the amine at the 3-position of the generated *o*-quinone species **11ox** or **18ox** (Scheme 8, step 1), but also facilitated α-proton abstraction and the subsequent electron flow from the α-carbon to the *o*-quinone moiety, which aromatizes to a Schiff base intermediate (Scheme 8, step 2). Crucial also was the presence of an active hydroxyl group at the 4-position, which was previously proved to be an essential requirement for the successful operation of the catalytic process in the studied series.[9c,10a-d,20] The activation of the imine function for further nucleophilic attack by the amine **15**, leading to the extrusion of imine **16** (Scheme 8, step 3), was provided by the intramolecular hydrogen bond between the 4-hydroxyl group and the imine nitrogen, generating a highly reactive H-bonded CTS.[9c,20c] Similar effects of phenolic hydroxyl groups on the reactivity of ketimine derivatives have been previously reported.[21] Aerobic oxidation of the generated aminophenol form **12red** or **23red** after single turnover generated the active *o*-iminoquinone organocatalyst (Scheme 8, step 4), which can undergo transamination with benzylamine substrate (Scheme 8, step 5) and close the catalytic cycle by passing **11ox** or **18ox**.

The bioinspired organocatalytic cascade reaction reported here allows the selective oxidation of primary amines to imines under ambient air, at room temperature, without any metal cocatalyst or additives. These environmentally mild conditions are particularly favourable for using the imine in situ for further reactions. Accordingly, we have focused on two synthetic applications, first, the oxidative cross-coupling of primary amines, second, the synthesis of 1,2-disubstituted benzimidazoles.

The oxidative cross-coupling of primary amines is known to be a challenging transformation as self-coupling is usually preferred. Recently, selective formation of cross-coupled imines has been reported, but the procedures generally require elevated temperature, oxygen pressure, metal cocatalyst, additive or problematic solvent.[10,22] Our dual bioinspired cascade reaction sequence proved to be effective for producing cross-coupling imines. The optimized reaction conditions we had previously reported[17] were applied by mixing two primary amines in a ratio 1:1 upon increasing pyrogallol **11red** loading to 10 mol% (generating 5 mol% of active organocatalyst **12ox**), in MeOH, at room temperature, under ambient air. Note MeOH was found to be the best solvent for the aerobic oxidative coupling of primary amines to imines because it provided the ideal balance of **11ox** (or **12ox**) solvation by enhancing the electrophilicity of the quinonoid moiety and reaction rate.[20,23] Although MeOH was initially considered as problematic according to Safety, Health and Environment (SH&E) criteria, it was finally ranked as recommended in the CHEM21 solvent guide.[24] The result of the **12ox**-mediated aerobic cross-coupling of primary amines is illustrated in Table 1 (See Experimental). The reaction is quite effective for various *sec*-primary amines **24a-l** and unbranched aliphatic primary amines **24m** and **24n**. A single colourless crystal of imine **24j** suitable for X-ray diffraction analysis was obtained from MeOH (Chart 1 and Table S1). Complete selectivity was observed except for cross-coupled imines **24m** and **24n** since the analysis of the reaction mixture by ^{1}H NMR revealed the presence of 7% of the corresponding homocoupled imine (See ESI). However, with poor nucleophilic 4-methoxyaniline, the conversion did not exceed 68% after 60h, leading to the cross-coupled imine **24o** in only 55% isolated yield.

More challenging, the possibility of expanding the reaction scope to the synthesis of scarcely stable aliphatic imines has also been explored. Due to their isomerization into enamine tautomer, which decomposes under ambient air, the generated alkylimines have been generally trapped in situ for further reactions.[10d,11g] So, we have performed the aerobic oxidative cross-coupling of a range of non-activated primary aliphatic amines with *N*-substituted-*o*-aminoanilines as in situ imine trap. This reaction led to 1,2-disubstituted benzimidazoles which are privileged and significant structural components of pharmaceuticals.[25] For this reason, numerous strategies have been developed for the regiocontrolled synthesis of 1,2-disubstituted benzimidazoles.[26] In particular, the catalytic oxidative coupling of amines has provided a straightforward protocol to synthesize substituted benzimidazoles derivatives through the variation of both commercially available cyclocondensation partners.[11a,c,d,f,27] However, with only few exceptions,[11a,c,d] the molecular diversity is limited to derivatives bearing benzylic or allylic substituents at the 2-position of the benzimidazole framework, because of the difficulty of oxidizing non-activated primary amines.

Table 1 **12ox**-mediated aerobic oxidative cross-coupling of amines[a]

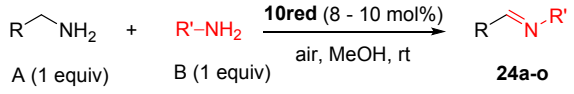

Amine A	Amine B	Cross-coupled imine	Yield (%)[b]
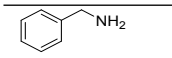	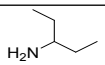	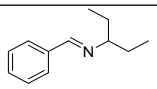	**24a** 85
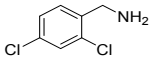		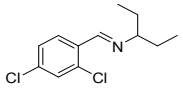	**24b** 87
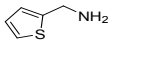		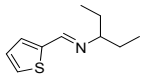	**24c** 83
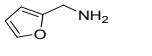		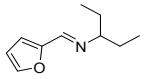	**24d** 89
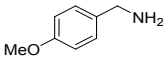	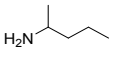	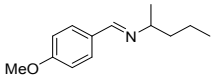	**24e** 89
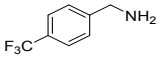	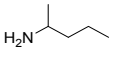	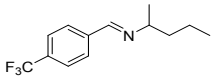	**24f** 90
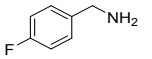	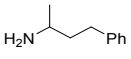	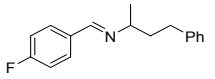	**24g** 88
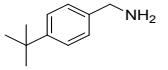	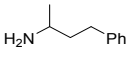	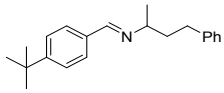	**24h** 84
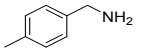	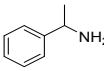	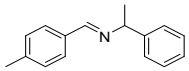	**24i** 90
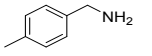	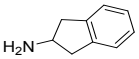	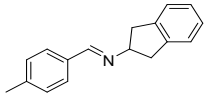	**24j** 90
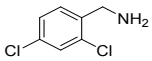	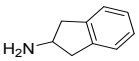	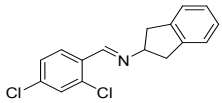	**24k** 80
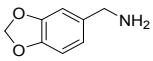	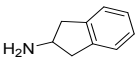	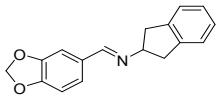	**24l** 89
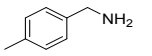	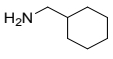	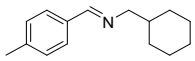	**24m** 93[c]
			24n 93[c]
			24o 55[d]

[a]8 mol% of **10red** affording 4 mol% of **12ox**, rt, 100% conversion, reaction times: 24h for **24a-c**, **24e**, **24f**, **24m** and **24n**; 48h for **24d** and 60h for **24g-l** and **24o**; additional aliquot of **10red** (2 mol%) was added after 24h. [b]Isolated yields after column chromatography. [c]Yields of the cross-coupled imine were determined by ^{1}H NMR. [d]68% conversion.

Table 2 Representative isolated 1,2-disubstituted benzimidazoles **25a-o**[a]

Amine A	Amine B	1,2-Benzimidazole	Yield (%)[b]
			25a 76
			25b 75
			25c 61
			25d 70
			25e 71[c]
			25f 64
			25g 63
			25h 67
			25i 62
			25j 74
			25k 52
			25l 40
			25m 75
			25n 76[c]
			25o 73[c]

[a]8 mol% of **10red** affording 4 mol% of **12ox**,100% conversion, reaction times 60h, 60°C for **25a-l**; 45°C for **25m-o**; additional aliquot of **10red** (2 mol%) was added after 24h. [b]Yields of the isolated product. [c]72h.

Under the optimized reaction conditions previously reported,[17] but at a slightly more elevated temperature of 60°C, the organocatalyst **12ox** was sufficiently reactive to activate the α-C-H bond of diverse non-activated primary aliphatic amines to give 1,2-disubstitued benzimidazoles **25a-j** in good isolated yields (Table 2 and Experimental). A single colourless crystal of benzimidazole **25d** suitable for X-ray diffraction analysis was obtained from the chloroform/petroleum ether solvent system (Chart 1 and Table S1). Note this reaction was unsuccessful in the absence of Cu (II) cooperative catalyst when **2** was used as the sole organocatalyst.[11c] As previously reported for catalysed aerobic oxidation of non-activated alcohol,[28] a decreased reactivity for sterically constrained β-branched alkylamines was observed affording the benzimidazoles **25k** and **25l** in 52 and 40% yields, respectively. As expected, the procedure could also be applied to common benzylic amines including heterocyclic amines containing a sulphur or oxygen atom which gave 1,2-disubstituted benzimidazoles **25n** and **25o** in good yields, after a prolonged reaction time of 72h.

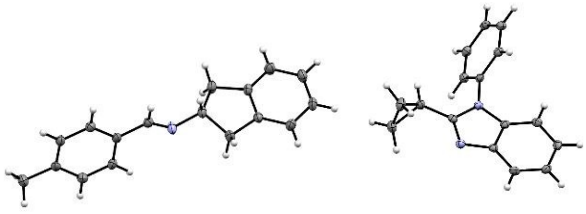

24j **25d**

Chart 1 Ortep views of imine **24j** and 1,2-benzimidazole **25d**. Displacement ellipsoids are drawn at the 50% probability level.

Finally, cross-coupled imines **24a-o** were obtained through the transamination mechanism reported in Scheme 8, yielding the homocoupled imine intermediate, which was progressively consumed in favour of the cross-coupled imine through dynamic transimination (Scheme 9, path 1).[10,17] Its formation could be driven by continuous oxidation of the extruded primary amine R-CH_2-NH_2 (self-sorting step) which was re-engaged in the transamination mechanism. So, just one equivalent of each amine was sufficient to achieve exclusive formation of the cross-coupled imine product. This oxidative strategy, known as oxidative self-sorting, has extensively been utilized to obtain thermodynamically disfavoured products. [29] In the presence of *o*-aminoanilines, the resulting cross-coupled imines were engaged in cyclocondensation and oxidation reaction steps to furnish 1,2-disubstituted benzimidazoles **25a-o** (Scheme 9, path 2).

Conclusion

New information about the reaction mechanism of an organocatalytic cascade reaction for the activation of the α-C-H bond of primary amines are disclosed through the isolation of [5 + 2] cycloaddition purpurogallin-like intermediates. The one pot protocol, mimicking both purpurogallin biosynthesis and CuAOs activity, utilizes inexpensive commercially available pyrogallol pre-catalyst, for delivering in situ, under ambient air, at room temperature, low loadings of the active biomimetic organocatalyst, which mediates the oxidative coupling of primary amines. Without any metal cocatalyst or additives, the method gives access to diverse cross-coupling imines, or 1,2-disubstituted benzimidazole derivatives in the presence of *o*-aminoanilines. This method constitutes an appropriate illustration of the potential of "second order" biomimicry in terms of atom economy, while preserving the benefit of the eco-friendly nature of the bioinspired catalytic processes. A rational application of this concept should allow the discovery of efficient catalysts generated from simple, low-cost precursors, introducing new opportunities in green chemistry.

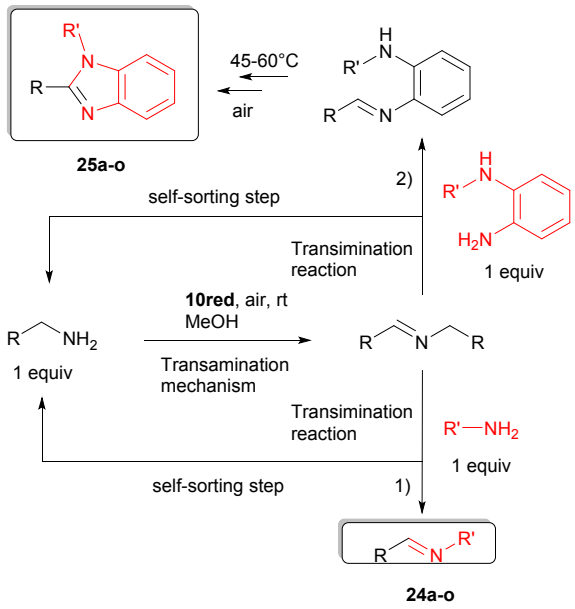

Scheme 9 Biomimetic cascade reaction sequence affording cross-coupled imines **24a-o** or 1,2-disubstituted benzimidazoles **25a-o**.

Experimental

Isolation of the [5 + 2] cycloaddition redox products 18red and 19red in the course of the aerobic oxidation of benzylamine 15 mediated by 17red

Benzylamine **15** (2 mmol) and pyrogallol derivative **17red** (0.5 mmol) were mixed in MeOH (25 mL), under ambient air. The reaction mixture was stirred at room temperature. The progress of the reaction was monitored by ^{1}H NMR spectroscopy. When 30% of benzylamine **15** was converted into *N*-benzylidene benzylamine **16**, the reaction was stopped by addition of dry ice. After evaporation of the solvent under reduced pressure at 30°C, the residue was purified by column chromatography (toluene-acetone, 90/10 v/v) on silica gel, to afford the [5+2] cycloaddition redox intermediates **18red** (0.025 mmol) and **19red** (0.075 mmol) in 5 and 15% yields, respectively. Caution: particular attention is required during the column chromatography which has to be realized quickly to minimize the aerobic oxidation of products **18red** and **19red** to melanin-like polymers.

View Article Online
DOI: 10.1039/C9GC03992A

1,7-dibenzyl-2,3,4,6-tetrahydroxy-5*H*-benzo[7]annulen-5-one (18red). Orange solid (10 mg, 5%): mp 172-176 °C; R_f = 0.5 (toluene-acetone, 80/20 v/v); ^{1}H NMR (300 MHz, DMSO D6) δ4.03 (s, 2H), 4.32 (s, 2H), 6.77 (d, *J* = 12.4 Hz, 1H), 7.08-7.26 (m, 10H), 7.49 (d, *J* = 12.4 Hz, 1H), 15.57 (s, 1H, D_2O exchanged); ^{13}C{^{1}H} NMR (75 MHz, DMSO D6) δ 31.4, 39.1, 115.9, 117.3, 126.1, 126.7, 128.26 (x2), 128.33, 128.68, 128.74 (x2), 128.88 (x2), 129.1 (x2), 130.1, 130.8, 134.8, 140.1, 141.0, 150.5, 151.2, 152.6, 182.1; HRMS (ESI-) *m/z* calcd for $C_{25}H_{20}O_5$ [M – H]$^-$ 399.1232. Found 399.1238. 1D and 2D NMR spectra for compound **18red** are reported in the ESI. Key HMBC correlations are shown in Chart 2.

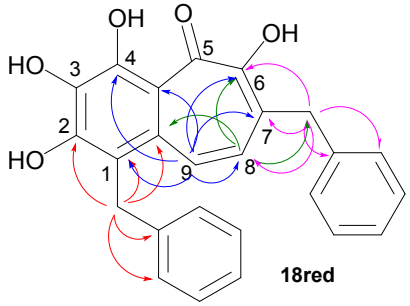

18red

Chart 2 Key HMBC correlations of compound **18red**.

(6R,9R)-1,7,11-tribenzyl-2,3,4,6-tetrahydroxy-6,9-dihydro-5*H*-6,9-(epiminomethano)benzo[7]annulene-5,10-dione (19red). Yellow crystal (40 mg, 15%): mp 244-248 °C; R_f = 0.4 (toluene-acetone, 80/20 v/v); ^{1}H NMR (400 MHz, CD_3OD) δ3.40-3.48 (m, 2H), 3.99 (d, *J* = 16.3 Hz, 1H), 4.48-4.56 (m, 3H), 4.82 (m, 1H), 5.54 (d, *J* = 7.0 Hz ,1H), 6.97 (m,2H), 6.96-7.189 (m, 13H); ^{13}C{^{1}H} NMR (100 MHz, CD_3OD) δ 30.3, 35.2, 43.2, 48.3, 87.8, 105.2, 118.6, 125.5, 125.9, 126.8, 127.5 (x2), 127.78 (x2), 127.82 (x2), 127.9 (x2), 128.0 (x2), 128.7, 128.8 (x2), 131.6, 131.8, 137.5, 137.6, 141.1, 145.6, 151.2, 153.5, 171.1, 191.9; HRMS (ESI-) *m/z* calcd for $C_{33}H_{27}NO_6$ [M – H]$^-$ 532.1760. Found 532.1772. X-Ray analysis: A yellow crystal of 0.27 × 0.22 × 0.05 mm, crystallized from a mixture toluene/methanol was used. Empirical formula $C_{33}H_{27}NO_6$, M = 533.55, T = 100(2) K. Triclinic system, space group P-1, *Z* = 4, *a* = 12.6327(6) Å, *b* = 15.2434(7) Å, *c* = 15.9800(7) Å, α = 102.027(2)°, β = 105.432(2)°, γ = 112.595(2)°, *V* = 2566.4(2) Å^3, d_{calc} = 1.381 g cm^{-3} , F(000) = 1120, μ = 0.776 mm^{-1}, λ(CuKα) = 1.54178 Å. 77250 intensity data were collected with a VENTURE PHOTON100 CMOS Bruker diffractometer (Cu-Kα radiation) controlled by APEX3 software package, giving 9064 unique reflections. Refinement of 743 parameters on F^2 led to $R_1(F)$ = 0.0375 calculated with 7934 observed reflections as $I \geq 2$ sigma (I) and $wR_2(F^2)$ = 0.1045 considering all the 9064 data. Goodness of fit = 1.011. CCDC deposition number: 1965257. 1D and 2D NMR spectra for compound **19red** are reported in the ESI. Key HMBC correlations are shown in Chart 3.

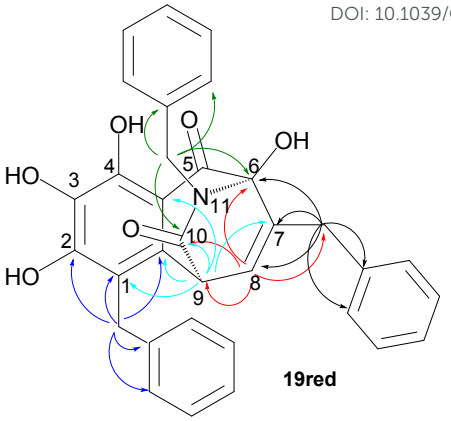

19red

Chart 3 Key HMBC correlations of compound **19red**.

Representative experimental procedure for the organocatalyzed aerobic oxidative cross-coupling of two primary amines

Equimolar amounts of benzylamine (2.5 mmol) and 1-ethylpropylamine (2.5 mmol), pyrogallol **10red** (0.2 mmol, 8 mol%, corresponding to the generation of 4 mol% of purpurogallin **11red**) were mixed in MeOH (10 mL), under ambient air. The reaction mixture was stirred at room temperature for 24h. The progress of the reaction was monitored by ^{1}H NMR spectroscopy. After completion of the reaction, the solvent was evaporated, at room temperature, to give the cross-coupling imine product **24a** as an almost pure product, which was further purified by washing through a small pad of base-washed silica (eluent: 1/2 petroleum ether/ethyl acetate + 2% triethylamine). Caution: particular attention is required during the column chromatography which has to be realized quickly to avoid the hydrolysis of the cross-coupled imine to aldehyde. The above procedure is generally representative for all the products shown in Table 1. Any deviations from this protocol are specified in the footnotes of Table 1.

X-Ray analysis of imine 24j. A colorless crystal of 0.23 × 0.19× 0.04 mm, crystallized from methanol was used. Empirical formula $C_{17}H_{17}N$, M = 235.1, T = 100(2) K. Triclinic system, space group P-1, Z = 2, *a* = 5.6742(2) Å, *b* = 8.7921(4) Å, *c* = 13.5713(5) Å, α = 103.259(1) °, β = 95.099(1)°, γ = 95.624(1)°, *V* = 651.48(4) Å^3, d_{calc} = 1.200 g cm^{-3} , F(000) = 252, μ = 0.526 mm^{-1}, λ(CuKα) = 1.54178 Å. 21496 intensity data were collected with a VENTURE PHOTON100 CMOS Bruker diffractometer (Cu-Kα radiation) controlled by APEX3 software package, giving 2166 unique reflections. Refinement of 166 parameters on F^2 led to R_1(F) = 0.0439 calculated with 1995 observed reflections as $I \geq 2$ sigma (I) and $wR_2(F^2)$ = 0.1122 considering all the 2166 data. Goodness of fit = 1.072. CCDC deposition number: 1981805.

View Article Online
DOI: 10.1039/D0GC03972A

General experimental procedure for the organocatalyzed aerobic oxidative coupling reaction affording 1,2-disubstituted benzimidazoles

Equimolar amounts of primary amine (1.25 mmol) and *N*-substituted-*o*-aminoaniline (1.25 mmol) with pyrogallol **10red** (0.1 mmol, 8 mol%, which corresponds to the generation of 4 mol% of purpurogallin **11red**), were mixed in MeOH (25 mL), in an air atmosphere. The reaction mixture was stirred at 60°C for 24h. Then, an additional aliquot of 0.025 mmol of **10red** (2 mol%) was introduced into the reaction mixture and the reaction was continued for 36h. The solvent was then removed by evaporation under reduced pressure, and the residue was purified by column chromatography on silica gel (eluent: 1/1 petroleum ether/ethyl acetate) to afford 1,2-disubstituted benzimidazoles **25a-o**. The above procedure is generally representative for all benzimidazoles shown in Table 2. Any deviations from this protocol are specified in the footnotes of Table 2.

X-Ray analysis of 1,2-benzimidazole 25 d. A colorless crystal of 0.21 × 0.16× 0.10 mm, crystallized from a mixture chloroform/petroleum ether was used. Empirical formula $C_{16}H_{14}N_2$, M = 234.29, T = 100(2) K. Triclinic system, space group P-1, *Z* = 4, *a* = 10.3880(4) Å, *b* = 10.8621(4) Å, *c* = 11.9356(4) Å, α = 103.368(1)°, β = 111.316(21)° , γ = 90.267(1)°, V = 1214.77(8) Å^3, d_{calc} = 1.281 g cm^{-3} , F(000) = 496, μ = 0.591 mm^{-1}, λ(CuKα) = 1.54178 Å. 29618 intensity data were collected with a VENTURE PHOTON100 CMOS Bruker diffractometer (Cu-Kα radiation) controlled by APEX3 software package, giving 3491 unique reflections. Refinement of 325 parameters on F^2 led to $R_1(F)$ = 0.0314 calculated with 3328 observed reflections as $I \geq 2$ sigma *(I)* and $wR_2(F^2)$ = 0.784 considering all the 3491 data. Goodness of fit = 1.099. CCDC deposition number: 1981802

Conflicts of interest

There are no conflicts to declare.

Acknowledgements

We thank CNRS and Paris Descartes University for financial support. Pascale Leproux is acknowledged for running high resolution mass spectra. The authors also wish to thank Regis Guillot (ICMMO – Université Paris Saclay) for collecting the crystallographic data.

Notes and references

1 For selected reviews or perspectives, see: *(a)* L. Marchetti and M. Levine, *ACS catal.* 2011, **1**, 1090; *(b)* C. K. Prier and F. H. Arnold, *J. Am. Chem. Soc.* 2015, **137**, 13992; *(c)* R. A. Sheldon and J. M. Woodley, *Chem. Rev.* 2018, **118**, 801; *(d)* R. A. Sheldon and D. Brady, *ChemSusChem.* 2019, **12**, 2859.

2 For selected reviews, see: *(a)* O. Pamies, M. Dieguez and J.-E. Bäckvall, *Adv. Synth. Catal.* 2015, **357**, 1567; *(b)* F. Schwizer, Y. Okamoto, T. Heinisch, Y. Gu, M. M. Pellizzoni, V. Lebrun, R. Reuter, V. Köhler, J. C. Lewis, T. R. Ward, *Chem. Rev.* 2018, **118**, 142; *(c)* M. T. Reetz, *Acc. Chem. Res.* 2019, **52**, 336; *(d)* E. N. Mirts, A. Bhagi-Damodaran and Y. Li, *Acc. Chem. Res.* 2019, **52**, 935.

3 For selected reviews, see: *(a)* J. Piera and J. E. Bäckvall, *Angew. Chem. Int. Ed.* 2008, **47**, 3506; *(b)* L. Que Jr and W. B. Tolman, *Nature*, 2008, **455**, 333; *(c)* L. Que Jr and W. N. Oloo, *Acc. Chem. Res.* 2015, **48**, 2612; *(d)* M. M. Pereira, L. D. Dias and M. J. F. Calvete, *ACS catal.* 2018, **8**, 10784.

4 For selected reviews, see: *(a)* J. P. Klinman, *Chem. Rev*. 1996, **96**, 2541; *(b)* J. P. Klinman, *Biochim. Biophys. Acta*, 2003, **1647**, 131; *(c)* B. J. Brazeau, B. J. Johnson and C. M. Wilmot, *Arch. Biochem. Biophys.*, 2004, **428**, 22; *(d)* P. Matyus, B. Dajka-Halasz, A. Földi, N. Haider, D. Barlocco, K. Magyar, *Curr. Med. Chem*. 2004, **11**, 1285; *(e)* M. Strolin Benedetti, K. F. Tipton and R. Whomsley, *Fondam. Clin. Pharmacol.*, 2007, **21**, 467; *(f)* A. Boobis, J. B. Watelet, R. Whomsley, M. Strolin Benedetti, P. Demoly and K. T. Tipton, *Drug Metab. Rev.*, 2009, **41**, 486.

5 S. M. Janes, D. Mu, D. Wemmer, A. J. Smith, S. Kaur, D. Maltby, A. L. Burlingame and J. P. Klinman, *Science*, 1990, **248**, 981.

6 S. Suzuki, T. Okajima, K. Tanizawa and M. Mure, Cofactors of amine oxidases. Copper ion and its substitution and the 2,4,5-trihydroxyphenylalanine quinone. In *Copper Amine Oxidases*. *Structures, Catalytic Mechanisms, and Role in Pathophysiology*, ed. G. Floris and B. Mondovi, CRC Press, Taylor and Francis Group Publishing, New York, 2009; p. 19.

7 *(a)* M. Mure, S. A. Mills and J. P. Klinman, *Biochemistry*, 2002, **41**, 9269-9278*; (b)* M. Mure, *Acc. Chem. Res.*, 2004, **37**, 131; *(c)* J. L. Dubois and J. P. Klinman, *Arch. Biochem. Biophys.*, 2005, **433**, 255; *(d)* J. P. Klinman and F. Bonnot, *Chem. Rev.* 2014, **114**, 4343.

8 For selected examples, see: *(a)* Y. Lee and L. M. Sayre, *J. Am. Chem. Soc.*, 1995, **117**, 3096; *(b)* M. Mure and J. P. Klinman, *J. Am. Chem. Soc.*, 1995, **117**, 8698; *(c)* M. Mure and J. P. Klinman, *J. Am. Chem. Soc.*, 1995, **117**, 8707; *(d)* Y. Lee and L. M. Sayre, *J. Am. Chem. Soc.*, 1995, **117**, 11823; *(e)* K. Q. Ling, J. Kim and L. M. Sayre, *J. Am. Chem. Soc.*, 2001, **123**, 9606; *(f)* M. Mure, S. X. Wang and J. P. Klinman, *J. Am. Chem. Soc.*, 2003, **125**, 6113.

9 For reviews or perspectives, see: *(a)* M. Largeron and M.-B. Fleury, *Science*, 2013, **339**, 43; *(b)* A. E. Wendlandt and S. S. Stahl, *Angew. Chem. Int. Ed.* 2015, **54**, 14638; *(c)* M. Largeron, *Org. Biomol. Chem.* 2017, **15**, 4722; *(d)* R. Zhang and S. Luo, *Chin. Chem. Lett.* 2018, **29**, 1193; *(e)* M. Largeron, *Pure Appl. Chem.* 2019, DOI: 10.1515/pac-2019-0107.

10 For selected recent examples, see: *(a)* A. E. Wendlandt and S. S. Stahl, *Org. Lett.* 2012, **14**, 2850; *(b)* M. Largeron and M.-B. Fleury, *Angew. Chem. Int. Ed.* 2012, **51**, 5409; *(c)* D. V. Jawale, E. Gravel, E. Villemin, N. Shah, V. Geersten, I. N. N. Namboothiri and E. Doris, *Chem. Commun.* 2014, **50**, 15251; *(d)* M. Largeron and M.-B. Fleury, *Chem.– Eur. J.*, 2015, **21**, 3815; *(e)* Y. Goriya, H. Y. Kim and K. Oh, *Org. Lett.* 2016, **18**, 5174; *(f)* R. Jangir, M. Ansari, D. Kaleeswaran, G. Rajaraman, M. Palaniandavar and R. Murugavel, *ACS Catal.* 2019, **9**, 10940.

11 For selected recent examples, see: *(a)* K. M. H. Nguyen and M. Largeron, *Chem.– Eur. J.*, 2015, **21**, 12606; *(b)* M. A. Leon, X. Liu, J. H. Phan and M. D. Clift, *Eur. J. Org. Chem.* 2016, **2016**, 4508; *(c)* K. M. H. Nguyen and M. Largeron, *Eur. J. Org. Chem.* 2016, **2016**, 1025; *(d)* R. Zhang, Y. Qin, L. Zhang and S. Luo, *Org. Lett.* 2017, **19**, 5629; *(e)* K. Kim, H. Y. Kim and K. Oh*, Org. Lett.* 2019, **21**, 6731; *(f)* S. A. Pawar, A. N. Chand, and A. Vijay Kumar, *ACS Sustainable Chem. Eng.* 2019, **7**, 8274; *(g)* Q. Yang, Y. Zhang, W. Zeng, Z.-C. Duan, X. Sang and D. Wang, *Green Chem.* 2019, **21**, 5683.

12 (a) R. Zhang, Y. Qin and S. Luo, *J. Org. Chem.* 2019, **84**, 2542. (b) B. Li, A. E. Wendlandt and S. S. Stahl, *Org. Lett.* 2019, **21**, 1176.

13 T. Si, H. Y. Kim and K. Oh, *ACS catal.* 2019, **9**, 9216.
14 (a) Y. Qin, L. Zhang, J. Lv, S. Luo and J.-P. Cheng, *Org. Lett.* 2015, **17**, 1469. (b) G. Golime, G. Bogonda, H. Y. Kim and K. Oh, *ACS catal.* 2018, **8**, 4986.
15 (a) H. Yuan, W.-J. Yoo, H. Miyamura and S. Kobayashi, *J. Am. Chem. Soc.* 2012, **134**, 13970. (b) A. E. Wendlandt and S. S. Stahl, *J. Am. Chem. Soc.* 2014, **136**, 506. (c) A. E. Wendlandt and S. S. Stahl, *J. Am. Chem. Soc.* 2014, **136**, 11910. (d) D. V. Jawale, E. Gravel, N. Shah, V. Dauvois, H. Li, I. N. N. Namboothiri and E. Doris, *Chem.–Eur. J.* 2015, **21**, 7039.
16 S. D. McCann, J. -P. Lumb, B. A. Arndtsen and S. S. Stahl, *ACS Cent. Sci.* 2017, **3**, 314.
17 M. Largeron and M. -B. Fleury, *Chem. –Eur. J.* 2017, **23**, 6763.
18 *(a)* W. Dürckheimer and E. F. Paulus, *Angew. Chem. Int. Ed.* 1985, **24**, 224; *(b)* P. Ellerbrock, N. Armanino, M.K. Ilg, R. Webster and D. Trauner, *Nat. Chem.* 2015, **7**, 879; *(c)* A. J. E. Novak, C. E. Grigglestone and D. Trauner, *J. Am. Chem. Soc.* 2019, **141**, 15515.
19 Y. Wang, J. P. Park, S. H. Hong and H. Lee, *Adv. Mater.* 2016, **28**, 9961.
20 *(a)* M. Largeron and M.-B. Fleury, *J. Org. Chem.*, 2000, **65**, 8874; *(b)* M. Largeron, A. Neudörffer and M.-B. Fleury, *Angew. Chem. Int. Ed.*, 2003, **42**, 1026; *(c)* M. Largeron, A. Chiaroni and M.-B. Fleury, *Chem.–Eur. J.*, 2008, **14**, 996.
21 *(a)* H. Miyabe, Y. Yamaoka, Y. Takemoto, *Synlett* 2004, 2597; *(b)* H. Miyabe, Y. Yamaoka, Y. Takemoto, *J. Org. Chem.* 2006, **71**, 2099.
22 For selected recent examples, see: *(a)* A. T. Murray, R. King, J. V. G. Donnelly, M. J. H. Dowley, F. Tuna, D. Sells, M. P. John and D. R. Carbery, *ChemCatChem* 2016, **8**, 510; *(b)* Y. R. Girish, R. Biswas and M. De, *Chem.–Eur. J.* 2018, **24**, 13871; *(c)* R.E. Rodriguez-Lugo, M. A. Chacon-Teran, S. De Leon, M. Vogt, A. J. Rosenthal and V.R. Landaeta, *Dalton Trans.* 2018, **47**, 2061; *(d)* S. Hazra, P. Pilania, M. Deb, A. K. Kushawaha and A. J. Elias, *Chem.–Eur. J.* 2018, **24**, 15766; *(e)* R. Brisar, F. Unglaube, D. Hollmann, H. Jiao and E. Esteban, *J. Org. Chem.* 2018, **83**, 13481; *(f)* C.-P. Dong, A. Uematsu, S. Kumazawa, Y. Yamamoto, S. Kodama, A. Nomoto, M. Ueshima and A. Ogawa, *J. Org. Chem.* 2019, **84**, 11562.
23 For another example where MeOH was shown to be an efficient solvent for enhancing the quinone reactivity, see: C. W. Anson, S. Ghosh, S. Hammes-Schiffer and S. S. Stahl, *J. Am. Chem. Soc.* 2016, **138**, 4186.
24 D. Prat, A. Wells, J. Hayler, H. Sneddon, C. R. McElroy, S. Abou-Shehada and P. J. Dunn, *Green Chem.* 2016, **18**, 288.
25 E. Vitaku, D.T. Smith and J. T. Njardarson, *J. Med. Chem.* 2014, **57**, 10257.
26 For reviews, see: *(a)* L.C. R. Carvalho, E. Fernandes and M. M. B. Marques, *Chem. – Eur. J.* 2011, **17**, 12544 and references therein; *(b)* S. Singhal, P. Khanna, S. S. Panda and L. Khanna, *J. Heterocyclic Chem.* 2019, **56**, 2702. For selected recent examples, see: *(c)* M. Pizzeti, E. De Luca, E. Petricci, A. Porcheddu and M. Taddei, *Adv. Synth. Catal.* 2012, **354**, 2453; *(d)* N. T. Jui and S. L. Buchwald, *Angew. Chem. Int. Ed.* 2013, **52**, 11624; *(e)* S. Kumar Alla, R. Kiran Kumar, P. Sadhu and T. Punniyamurthy, *Org. Lett.* 2013, **15**, 1334; *(f)* D. Kommi, P. D. Jadhavar, D. Kumar and A. K. Chakraborti, *Green Chem.* 2013, **15**, 798; *(g)* J. -P. Lin, F. -H. Zhang, and Y. -Q. Long, *Org. Lett.* 2014, **16**, 2822; *(h)* L. Q. Tran, J. Li and L. Neuville, *J. Org. Chem.* 2015, **80**, 6102; *(i)* X. Shi, J. Guo, J. Liu, M. Ye and Q. Xu, *Chem. – Eur. J.* 2015, **21**, 9988; *(j)* H. Sharma, N. Kaur, N. singh and D. O. Jang, *Green Chem.* 2015, **17**, 4263; *(k)* Y.- L. Lai, J. -S. Ye and J. -M. Huang, *Chem. –Eur. J.* 2016, **22**, 5425; *(l)* J. Xia, X. Yang, Y. Li and X. li, *Org. Lett.* 2017, **19**, 3243; *(m)* C. Xie, X. Han, J. Gong, D. Li and C. Ma, *Org. Biomol. Chem.* 2017, **15**, 5811. *(n)* T. Liang, Z. Tan, H. Zhao, X. Chen, H. Jiang and M. Zhang, *ACS Catal.* 2018, **8**, 2242; *(o)* A. Bera, M. Sk, K. Sigh and D. Banerjee, *Chem. Commun.* 2019, **55**, 5958; *(p)* G. Lu, N. Luo, F. Hu, Z. ban, Z. Zhan and G.-S. Huang, *Adv. Synth. Catal.* 2019, DOI:10.1002/adsc.201901161.
27 For a recent review, see: M. Largeron and K. M. H. Nguyen, *Synthesis*, 2018, **50**, 241 and references therein.
28 B. Xu, J. -P. Lumb and B. A. Arndtsen, *Angew. Chem. Int. Ed.* 2015, **54**, 4208.
29 For a review, see: M. E. Belowich and J. F. Stoddart, *Chem. Soc. Rev.* 2012, **41**, 2003.

Journal Name ARTICLE

Table of contents entry

View Article Online
DOI: 10.1039/C9GC03992A

Low-cost pyrogallol precatalyst undergoes an oxidative self-processing step for delivering the active organocatalyst in situ through a dual biomimetic process.